Boosting the performance of formic acid microfluidic fuel cell

Boosting the performance of formic acid microfluidic fuel cell: Oxygen annealing enhanced Pd@graphene electrocatalyst

Dawei Li [a], Hong Xu [a], Li Zhang [a], Dennis Y.C. Leung [c], Filipe Vilela [b], Huizhi Wang [b], Jin Xuan [a, b,*]

[a] State-Key Laboratory of Chemical Engineering, School of Mechanical and Power Engineering, East China University of Science and Technology, Shanghai 200237, China

[b] School of Engineering & Physical Sciences, Heriot-Watt University, Edinburgh EH14 4AS, United Kingdom

[c] Department of Mechanical Engineering, The University of Hong Kong, Pokfulam Road, Hong Kong

*Corresponding author, Tel: +44 (0) 131 451 3293; Fax: +44 (0) 131 451 3129; email address: j.xuan@hw.ac.uk

Abstract: A new oxygen-annealing treatment for Pd supported on graphene was employed to enhance the electro-catalytic performance in formic acid microfluidic fuel cells. Experiments show that both the electro-oxidation reactivity and CO tolerance of the annealed catalyst are significantly improved. When testing the fuel cell, the maximum power density with annealed catalyst is 41% higher than the unannealed Pd@graphene catalyst, and 85% higher than Pd@VulcanXC-72. This enhancement is attributed to the Pd-O bond formation during the oxygen annealing step, which induces greater CO electro-oxidation reactivity.

Key words: Fuel cell; graphene; annealing; CO tolerance

1. Introduction

Formic acid microfluidic fuel cells (FAMFC) are promising power sources for portable devices and microelectronics because of their intrinsic non-toxic, high power density, with added suitability for storage and transportation [1-3]. FAMFC employs a membraneless design under laminar flow microfluidics, which conveys additional benefits including lower cost and improved heat/mass transport. Since FAMFC suffers negligible crossover and mass transfer limitations, their performances strictly depend on the electrode kinetics [4]. Therefore, development of new electro-catalytic materials will be crucial to further FAMFC R&D towards higher power density and stability.

In the past few years, although catalysts for formic acid anode in FAMFCs have been greatly improved, they have yet to reach satisfactory performances. One negative factor relates to the fact that poor initial catalytic reactivity remains a challenge. Although many new materials have been applied to improve formic acid oxidation (FAO) activity, such as metal/oxides alloys/carbides [5-7] and alternative supporting materials [8-10], such as activated carbon/CNT/graphene and modification of these carbon materials [11], the reactivities are still far from ideal. Another problem arises from the the CO intermediates of FAO cause poisoning of noble-metal electro-catalyst, leading to stability issues during long-term operation of FAMFC [12]. Although many of recent studies have shown to reduce the formation of CO intermediates, the overall progress are still not satisfied [12, 13]. Among the different noble metals studied, Pd-based electro-catalysts are regarded to be most suitable for FAO because they can

promote the direct pathway of conversion and decrease the generation of CO intermediates [13].

Recently, graphene has been recognized as a promising support material for electro-catalysts. Graphene-based catalysts show great initial performance in FAO, mainly attributed to graphene's two-dimensional structure and ultra-high conductivity [14]. Graphene provides a great surface area favorable for the dispersion of Pd particles, which greatly enhances the desired initial performance [14]. Nevertheless, the performance loss caused by CO poison is still a detrimental factor in Pd@graphene catalysts, which leads to cell degradation over a long-term operation. Some studies have shown that when carbon supports are annealed in different atmospheres, properties of the electro-catalysts could be greatly improved, particularly their tolerance to CO [15, 16]. Although various studies on the annealing treatment of carbon-supported materials can be found, to the best of our knowledge, there are no reports on oxygen annealing of graphene-based electro-catalysts available in literature. Due to the unique surface properties of graphene over other carbon materials, developing a suitable oxygen-annealing process is challenging. For example, various functional groups and organic-inorganic bonds on graphene can be readily over-oxidized in an oxygen-rich atmosphere, leading to dramatic performance loss. Therefore, the protocol developed for other carbon materials, e.g. oxygen annealing process for Pd @ Vulcan XC-72 [13], may not be fully suited for graphene-based materials. An optimized and tailored methodology is required for the treatment of graphene based electro-catalysts, which, this study aims to address.

In this manuscript, and for the first time, an oxygen annealing process is presented for graphene supported Pd electro-catalysts with a set target to boost the FAMFC performance and CO tolerance. The annealing process is tailored and optimized to ensure the enhancement of Pd electro-catalytic activity without weakening graphene's role as a supporting material. According to electrochemical characterization, Pd supported on graphene synthesized *via* hydrothermal method shows great electrocatalytic activity as well as CO tolerance after oxygen annealing, leading to 85% increase in the FAMFC performance.

2. Experimental

Graphene oxide (GO) were made from natural graphite powder via a modified Hummer's method producing a 1 mg ml^{-1} solution after washing with deionized water until pH-neutral [17]. Synthesis of Pd supported on graphene was conducted as follows. 3 ml of 10 mM $PdCl_2$ in HCl was added into 20 ml GO solution, and the pH was adjusted to 10, followed by ultrasonication for 30 min. The mixture was then poured into a 100ml Teflon autoclave and reacted in an oven under a temperature of 120 ^oC for 10 hours. The resulting solid precipitates were filtered and washed with ethanol and deionized water several times, then dried in a freeze drier before further processing. The catalyst (marked as Pd/G) was then further annealed under an O_2 atmosphere at 100 ^oC for 12 hours. The annealing temperature and duration were determined by optimization studies tailored for graphene-based materials, where thermogravimetric

(TG) experiments were adopted. According to the TG results and subsequent electrochemical experiments, the annealing temperature was set at 100 ^{o}C. The annealed catalyst was marked as Pd/G-O. Pd supported on VulcanXC-72 carbon powder was also synthesized under the same conditions as a control material (marked as Pd/VulcanXC-72). The Pd loading of all samples were measured to be 3% wt. (±0.5%).

The FAMFC were fabricated following the general procedures as specified in our previous work [18]. The assembly and working principle of the FAMFC are shown in Fig. 1a and b respectively. The poly(methyl methacrylate) and poly(vinyl chloride) layers were machined by a CO_2 laser fabricator (Universal Laser Systems). The sizes of the microchannels were 15 mm × 3 mm × 0.5 mm (L ×W× H) with reactive areas at anode and cathode to be 3 mm × 3 mm. The catalyst on cathode gas diffusion electrode (GDE) was 2 mg cm^{-2} Pt/C (Hesen), and the catalyst on the anode GDE was 2 mg cm^{-2} materials developed in this study (i.e. Pd/G-O, Pd/G and Pd/VulcanXC-72).

All electrochemical measurements were carried out on an electrochemical workstation (CHI660E). Cyclic voltammetry (CV) was performed in 0.5M HCOOH + 0.5M H_2SO_4 solutions with a three-electrode system from -0.2V to 1.0V at a scan rate of 50mVs^{-1}. The reference electrode was Ag/AgCl in saturated KCl (0.198V vs. SHE), and the counter electrode was a platinum film electrode (1 cm^2). Before electrochemical tests, the solutions were deaerated with nitrogen for 15 minutes. The CO-stripping experiment was conducted in a 0.5M H_2SO_4 solution with the same setup. Prior to the experiment, CO was purged into the electrolyte for 15 minutes for CO adsorption onto

the catalyst while the working electrode was kept at 0.2 V vs Ag/AgCl. After that, the excess CO was driven out with nitrogen for 15 minutes [19]. To evaluate the performance of the fuel cells, the anolyte (0.5M H_2SO_4 + 0.5M HCOOH) and catholyte (0.5M H_2SO_4) were pumped at 100 µl min^{-1} via a syringe pump (LSP02-1B). A potentiostatic method was performed at different potentials from 0.7V to 0V with 0.04V interval to obtain polarization curve. The electrochemical data was recorded when the potentiostatic current becomes stable after 100s.

The morphology and structural data of catalysts were determined by transmission electron microscope (TEM, Tecnai G2 F20) operated at an accelerating voltage of 200kV. The X-ray diffraction (XRD) patterns were carried out on Rigaku D/max-2550VB+/PC diffractometer using Cu KαD/max-2550. The X-ray photoelectron spectroscopy (XPS) measurements were performed on a SKL-12 multi-technique surface analysis system using Mg Kα radiation.

3. Results and discussion

XRD patterns of the three electro-catalyst materials, i.e. Pd/VulcanXC-72, Pd/G and Pd/G-O are compared in Fig. 1c to identify the Pd and graphene phase and crystal structure transformation during annealing. The diffraction peaks observed at 39.9°, 46.5° and 67.8° correspond to (111), (200) and (220) crystalline planes of the face centered cubic structured palladium (JCPDS No. 46-1043) and peaks at 25.0° corresponds to (002) crystalline plane of carbon (JCPDS No. 26-1077). It is found that

after annealing, the peaks of Pd/G-O become sharper when compared with Pd/G catalyst. The Pd grain size in Pd/G-O and Pd/G are calculated to be 5.0 nm and 4.4 nm, respectively, by the Scherer formula assigned to peaks of Pd (111) [20]. The phenomenon reveals that the Pd grain size is unaffected during the annealing treatment.

To further understand the effect to Pd particles from oxygen annealing, TEM was carried out to compare the morphologies of the materials (Fig.1 d and e). The supported graphene shows a reasonable plane structure. It also demonstrates that Pd nanoparticles do not aggregate with our optimized oxygen annealing parameters and conditions.

The catalysts performances in FAO are determined by electrochemical experiments in a three-electrode system. As a common protocol [21], the measured current is normalized by electrochemical surface area (ECSA), determined by the CO stripping experiment. Figure 2a shows the CV curves of Pd/VulcanXC-72, Pd/G and Pd/G-O catalysts in 0.5M H_2SO_4 solution for confirmation of the presence of Pd on the glassy carbon electrode. As it can be seen, the Pd-rich electrodes are confirmed by the existence of hydrogen adsorption/desorption peaks and reduction peaks of Pd oxides [22]. The CVs of FAO are then operated in 0.5M HCOOH solution, and the results are shown in Fig. 2b. The peak current density of Pd/G-O (1.38 mA cm^{-2}) is almost 156% higher than Pd/VulcanXC-72, and 100% higher than Pd/G. Furthermore, the FAO peak of Pd/G-O is observed at ~0.20V, which is 80mV more negative than that of Pd/VulcanXC-72. In addition, the shoulder peak in Pd/G could be attributed to the generation of new active sites between Pd and the graphene supports [23]. In Pd/G-O, the shoulder peak become less obvious. This is due to the increase in the area of the

main peak, and also because the shoulder peak sits very close to the main peak. The results indicate that Pd/G-O show significantly enhanced FAO activity, with the performance order of Pd/G-O> Pd/G> Pd/VulcanXC-72.

The CO stripping results are shown in Fig. 2c and d. It was found that the Pd/G-O shows the most activity to CO electro-oxidation, as the peak potential of Pd/G-O (0.75V) shifts negatively by about 30 mV and 20 mV compared to Pd/VulcanXC-72 and Pd/G, respectively. This can be attributed to the formation of the Pd-O bond, resulting in an easier electro-oxidization and removal at the Pd active sites [24]. It was also found that the CO electro-oxidation peak of Pd/G-O is much sharper, which indicates that CO electro-oxidation occurs in a narrower potential range with a faster reaction rate [25]. The CO stripping results indicate that our optimized oxygen annealing process could also largely increase the CO tolerance of the Pd@graphene catalyst.

The mechanism of electro-catalysis enhancement by oxygen annealing is further explained by XPS experiments (Fig. 3). In the XPS spectrum of C 1s (Fig. 3a), the C 1s gives three contributions observed at 284.60 eV, 285.96 eV, and 288.81 eV, which are corresponding to the sp^2 C=C, C-OH, and O-C=O [26]. No obvious peaks shift can be found in the C 1s spectrums before and after annealing, indicating that the physicochemical propoties of graphene carbon support remains almost unchanged during the heat treatment process. The results proves that the heating-induced graphene surface and structural destruction can be effectively prevented by the relatively low annealing temperature being carefully chosen in this study. Furthermore, according to the contributions, the amount of O-C=O is 10.4% in Pd/G-O catalyst, which is 3.3%

lower than Pd/G (13.7%). At the same time, the amount of sp^2 C=C is 59.7% in Pd/G-O catalyst, 4.4% higher than that in Pd/G. The reduction of O-C=O amount can be attributed to the fact that it will be oxidized on graphene surface during annealing process, which is expected to achieve a positive effect on graphene's electric conditivity [27]. On the other hand, for the Pd/G catalyst, (in the XPS spectrum of Pd 3d), the peaks at 335.31 eV and 340.56 eV are related to metallic Pd, and 335.89 eV and 341.35 eV are related to Pd-O bond. For Pd/G-O, the metallic Pd peaks shift to lower binding energy (335.04 eV and 340.36 eV), and Pd-O peaks shift to higher binding energy (336.22 eV and 341.99 eV), indicating the decrease of Pd-O electron density and increase in metallic Pd electron density [28]. This is because some Pd atoms combine with oxygen atoms, and electrons are transferred from Pd-O groups to Pd groups during the annealing process. An increase in 7% of Pd-O binding (from 45% to 52%) is found in the XPS spectrum after annealing. According to previous studies [29, 30], Pd-O groups mainly exist on the surface, and the surface Pd-O groups exhibit high activity to CO oxidation, because the palladium atoms that adjacent to the oxygen atoms show a lower activation energy. In addition, the surface oxygen atoms is also in favor of regenerating catalytic surface, which could maintain the electro-activity. This indicates CO intermediates adsorbed on the active sites could be removed more quickly than Pd atoms without oxygen atom revolved. Therefore, the additional Pd-O groups formed in our optimized annealing process is the main driver in the enhancement of CO electro-oxidation activities, in which the properties of graphene remains unchanged.

The developed catalytic materials were then tested in our FAMFC platform for comparison (Fig.4 a). The maximal cell power density with Pd/G-O, Pd/G and Pd/VulcanXC-72 is 15.2 mW cm^{-2}, 10.7 mW cm^{-2} and 8.3 mW cm^{-2}, respectively, proving that 41% performance increase can be induced by oxygen-annealing of Pd@graphene materials. The Pd/G-O cell also shows 85% higher performance than the electrocatalyst using conventional materials (Pd/VulcanXC-72). To further study the anode and cathode behaviors separately (Fig 4 b), an Ag/AgCl reference electrode is coupled in the FAMFC system, similar to our previous experimental setup [18]. Not surprisingly, the cathode polarization behaviors in the three cells are almost identical when the commercial catalyst was used. On the other hand, the Pd/G-O anode achieved significantly lower polarization loss than the other two anodes, which, therefore, can be inferred as the main reason for cell performance enhancement. It is noted that at high current operating range, the anode side trends to exhibit a limiting current behavior and the polarization curve even bends to a reverse direction. This is a normal phenomenon in FAMFC and can be found in many other studies [3, 31, 32], which is attributed to mass transfer limitation caused by low concentration of FA in higher current density and the increase in CO_2 bubbles generation. The limiting current behavior can be prevented by advanced cell designs but it is outside the scope of the present study. The full cell test results also indicate that the Pd-O bond formation not only improves the FAO, but also the activity of CO electro-oxidation, which contributes to the additional current harvested by the FAMFC.

4. Conclusions

This paper reports for the first time an optimized and tailored oxygen annealing process for graphene supported Pd electro-catalyst, which boosts the FAMFC performance and CO tolerance. The annealed Pd catalyst shows good electro-catalysis to FAO and great tolerance to CO. This is due to the Pd-O formation during the annealing in oxygen, which is favorable for CO electro-oxidization, while the annealing process does not affect the properties of the graphene supports. The high CO tolerance also signposts great potential for minimizing the electrode degradation issues during the FAMFC operation [11]. The oxygen-annealing method for graphene supported electrocatalyst developed in this study could provide a viable and cost-effective solution to the commercialization of FAMFC.

Acknowledgments

This work is supported by National Natural Science Foundation of China (51406057) and RGC/SFC Hong Kong-Scotland Collaborative Research Program (X-HKU710/14, H15009).

Notes and references

[1] Ha S, Larsen R, Zhu Y, Masel RI. Direct Formic Acid Fuel Cells with 600 mA cm^{-2} at 0.4 V and 22 °C. Fuel Cells. 2004;4:337-43.

[2] Rice C, Ha S, Masel RI, Waszczuk P, Wieckowski A, Barnard T. Direct formic acid fuel cells. Journal of Power Sources. 2002;111:83-9.

[3] Moreno-Zuria A, Dector A, Cuevas-Muñiz FM, Esquivel JP, Sabaté N, Ledesma-García J, et al. Direct formic acid microfluidic fuel cell design and performance evolution. Journal of Power Sources. 2014;269:783-8.

[4] Rhee Y-W, Ha SY, Masel RI. Crossover of formic acid through Nafion® membranes. Journal of Power Sources. 2003;117:35-8.

[5] Yang F, Zhang Y, Liu P-F, Cui Y, Ge X-R, Jing Q-S. Pd–Cu alloy with hierarchical network structure as enhanced electrocatalysts for formic acid oxidation. International Journal of Hydrogen Energy. 2016;41:6773-80.

[6] Hao Y, Shen J, Wang X, Yuan J, Shao Y, Niu L, et al. Facile preparation of PdIr alloy nano-electrocatalysts supported on carbon nanotubes, and their enhanced performance in the electro-oxidation of formic acid. International Journal of Hydrogen Energy. 2016;41:3015-22.

[7] Şener T, Demirci UB, Gül ÖF, Ata A. Pd–MnO_2–Fe_2O_3/C as electrocatalyst for the formic acid electrooxidation. International Journal of Hydrogen Energy. 2015;40:6920-6.

[8] Martins CA, Fernández PS, de Lima F, Troiani HE, Martins ME, Arenillas A, et al. Remarkable electrochemical stability of one-step synthesized Pd nanoparticles supported on graphene and multi-walled carbon nanotubes. Nano Energy. 2014;9:142-51.

[9] Jin T, Guo S, Zuo J-l, Sun S. Synthesis and assembly of Pd nanoparticles on graphene for enhanced electrooxidation of formic acid. Nanoscale. 2013;5:160-3.

[10] Wang Y, Zhao H, Tang Q, Zhang H, Li CM, Qi T. Electrocatalysis of titanium suboxide-supported Pt–Tb towards formic acid electrooxidation. International Journal of Hydrogen Energy. 2016;41:1568-73.

[11] Guo CX, Zhang LY, Miao J, Zhang J, Li CM. DNA-Functionalized Graphene to Guide Growth of Highly Active Pd Nanocrystals as Efficient Electrocatalyst for Direct Formic Acid Fuel Cells. Advanced Energy Materials. 2013;3:167-71.

[12] Capon A, Parsons R. The oxidation of formic acid on noble metal electrodes: II. A comparison of the behaviour of pure electrodes. Journal of Electroanalytical Chemistry and Interfacial Electrochemistry. 1973;44:239-54.

[13] Yu X, Pickup PG. Mechanistic study of the deactivation of carbon supported Pd during formic acid oxidation. Electrochemistry Communications. 2009;11:2012-4.

[14] Huang X, Qi X, Boey F, Zhang H. Graphene-based composites. Chemical Society Reviews. 2012;41:666-86.

[15] Yan L, Yao S, Chang J, Liu C, Xing W. Pd oxides/hydrous oxides as highly efficient catalyst for formic acid electrooxidation. Journal of Power Sources. 2014;250:128-33.

[16] She Y, Lu Z, Fan W, Jewell S, Leung MKH. Facile preparation of PdNi/rGO and its electrocatalytic performance towards formic acid oxidation. Journal of Materials Chemistry A. 2014;2:3894-8.

[17] Hummers WS, Offeman RE. Preparation of Graphitic Oxide. Journal of the American Chemical Society. 1958;80:1339-.

[18] Wang Y, Leung DYC, Xuan J, Wang H. A vapor feed methanol microfluidic fuel cell with high fuel and energy efficiency. Applied Energy. 2015;147:456-65.

[19] Zhou W, Lee JY. Particle Size Effects in Pd-Catalyzed Electrooxidation of Formic Acid. The Journal of Physical Chemistry C. 2008;112:3789-93.

[20] Yang J, Tian C, Wang L, Fu H. An effective strategy for small-sized and highly-dispersed palladium nanoparticles supported on graphene with excellent performance for formic acid oxidation. Journal of Materials Chemistry. 2011;21:3384-90.

[21] Ma A, Zhang X, Wang X, Le L, Lin S. Green synthesis of PdCu supported on graphene/polyoxometalate LBL films for high-performance formic acid oxidation. RSC Advances. 2015;5:64534-7.

[22] Zhang Y, Wang Y, Jia J, Wang J. Electro-oxidation of methanol based on electrospun PdO–Co_3O_4 nanofiber modified electrode. International Journal of Hydrogen Energy. 2012;37:17947-53.

[23] Chang J, Li S, Feng L, Qin X, Shao G. Effect of carbon material on Pd catalyst for formic acid electrooxidation reaction. Journal of Power Sources. 2014;266:481-7.

[24] Maillard F, Schreier S, Hanzlik M, Savinova ER, Weinkauf S, Stimming U. Influence of particle agglomeration on the catalytic activity of carbon-supported Pt nanoparticles in CO monolayer oxidation. Physical Chemistry Chemical Physics. 2005;7:385-93.

[25] Chang J, Sun X, Feng L, Xing W, Qin X, Shao G. Effect of nitrogen-doped acetylene carbon black supported Pd nanocatalyst on formic acid electrooxidation. Journal of Power Sources. 2013;239:94-102.

[26] Qian H, Huang H, Wang X. Design and synthesis of palladium/graphitic carbon nitride/carbon black hybrids as high-performance catalysts for formic acid and methanol electrooxidation. Journal of Power Sources. 2015;275:734-41.

[27] Ambrosi A, Bonanni A, Sofer Z, Cross JS, Pumera M. Electrochemistry at Chemically Modified Graphenes. Chemistry – A European Journal. 2011;17:10763-70.

[28] Casella IG, Contursi M. An electrochemical and XPS study of the electrodeposited binary Pd–Sn catalyst: The electroreduction of nitrate ions in acid medium. Journal of Electroanalytical Chemistry. 2006;588:147-54.

[29] Hirvi JT, Kinnunen T-JJ, Suvanto M, Pakkanen TA, Nørskov JK. CO oxidation on PdO surfaces. The Journal of Chemical Physics. 2010;133:084704.

[30] Li Y, Yu Y, Wang J-G, Song J, Li Q, Dong M, et al. CO oxidation over graphene supported palladium catalyst. Applied Catalysis B: Environmental. 2012;125:189-96.

[31] Chen F, Chang M-H, Lin M-K. Analysis of membraneless formic acid microfuel cell using a planar microchannel. Electrochimica Acta. 2007;52:2506-14.

[32] Zhang B, Ye D, Li J, Zhu X, Liao Q. Electrodeposition of Pd catalyst layer on graphite rod electrodes for direct formic acid oxidation. Journal of Power Sources. 2012;214:277-84.

List of Figures

Fig. 1

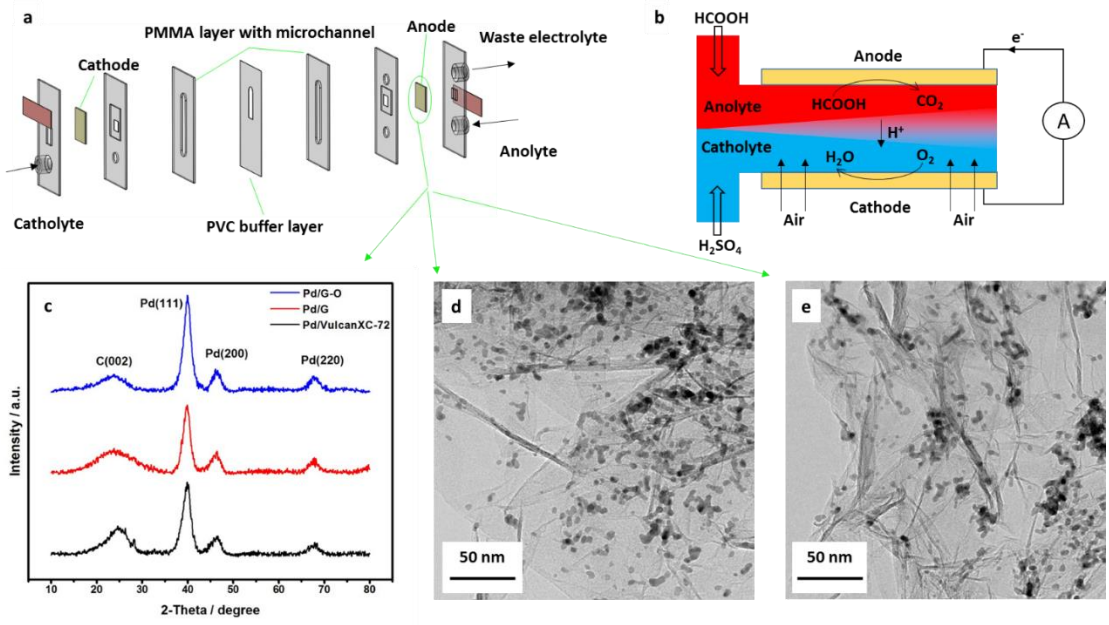
a
PMMA layer with microchannel
Anode
Waste electrolyte
Cathode
Anolyte
Catholyte
PVC buffer layer
b
HCOOH
Anode
e⁻
Anolyte
HCOOH
CO2
H+
Catholyte
H2O
O2
A
Air
Cathode
Air
H2SO4
c
Pd/G-O
Pd/G
Pd/VulcanXC-72
Pd(111)
C(002)
Pd(200)
Pd(220)
Intensity / a.u.
10
20
30
40
50
60
70
80
2-Theta / degree
d
50 nm
e
50 nm

Fig. 2

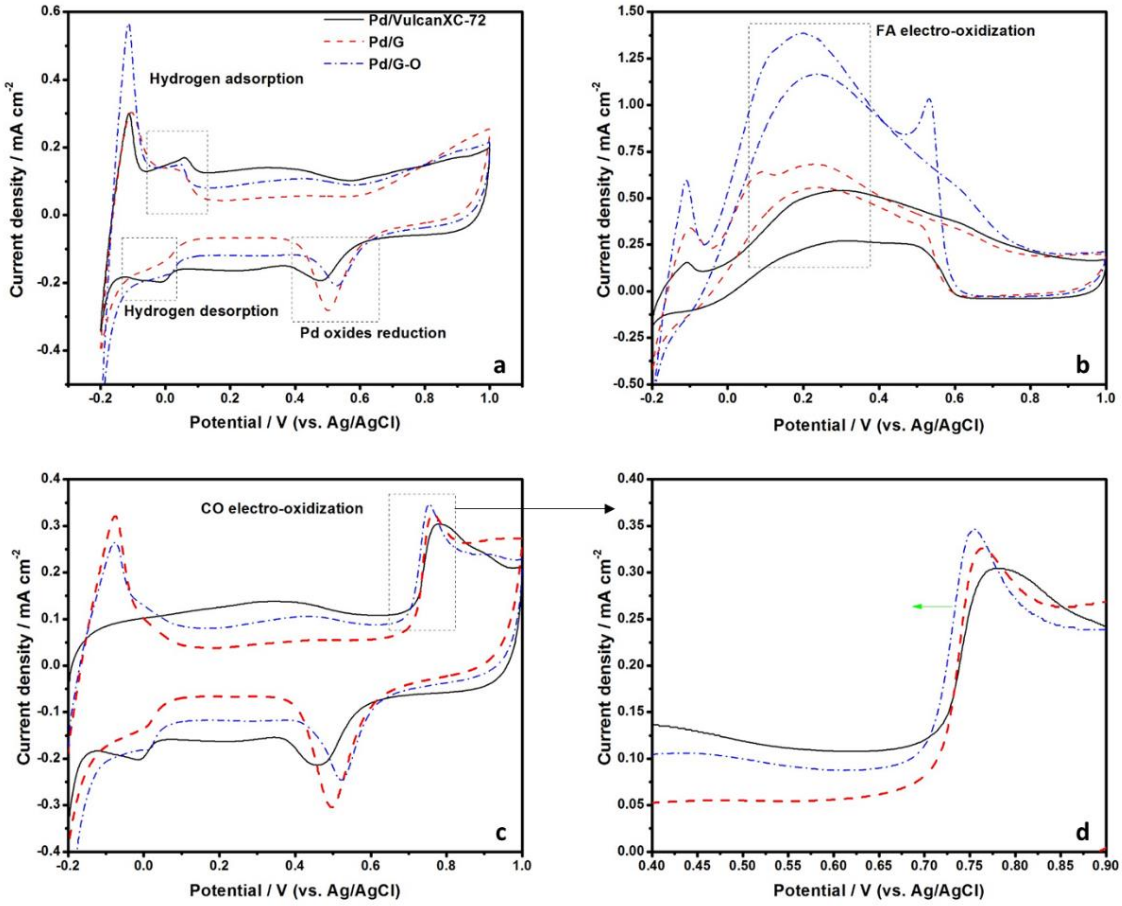
Pd/VulcanXC-72
Pd/G
Pd/G-O
Hydrogen adsorption
Hydrogen desorption
Pd oxides reduction
a
Current density / mA cm-2
Potential / V (vs. Ag/AgCl)
FA electro-oxidization
b
CO electro-oxidization
c
d

Fig 3

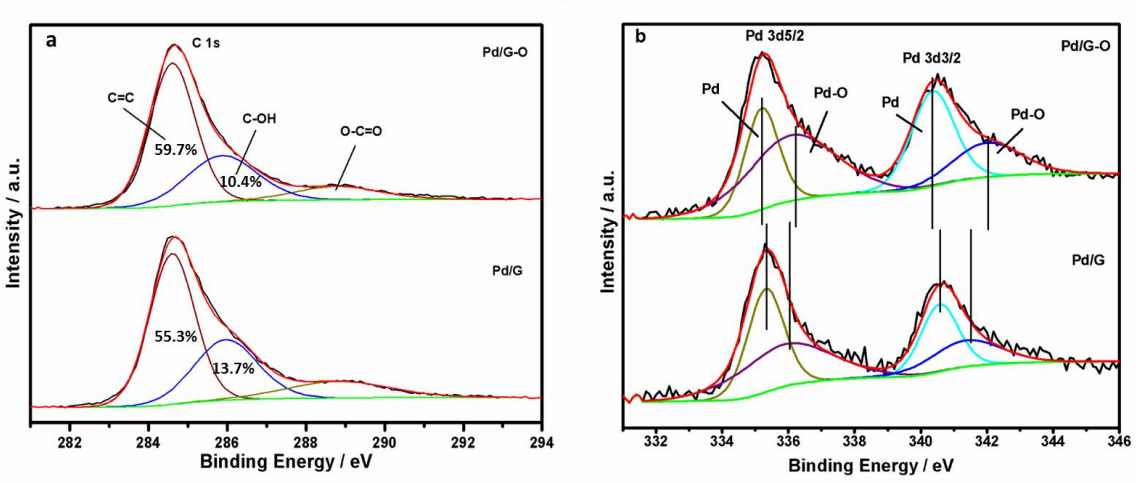
a
C 1s
Pd/G-O
C=C
C-OH
O-C=O
59.7%
10.4%
Pd/G
55.3%
13.7%
Intensity / a.u.
282
284
286
288
290
292
294
Binding Energy / eV
b
Pd 3d5/2
Pd 3d3/2
Pd/G-O
Pd
Pd-O
Pd
Pd-O
Pd/G
Intensity / a.u.
332
334
336
338
340
342
344
346
Binding Energy / eV

Fig. 4

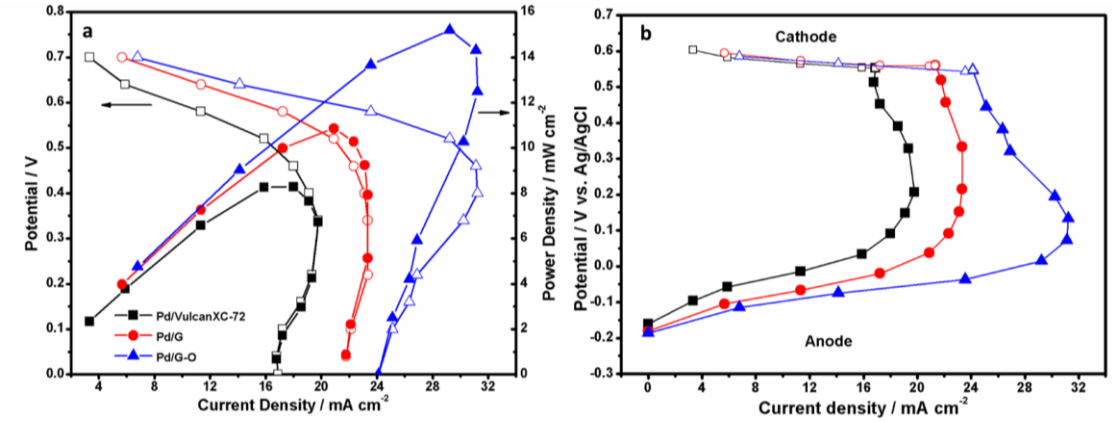
a
Potential / V
Power Density / mW cm-2
Current Density / mA cm-2
Pd/VulcanXC-72
Pd/G
Pd/G-O
b
Cathode
Anode
Potential / V vs. Ag/AgCl
Current density / mA cm-2